

Fig. 2 UV-Vis absorption (ABS) spectra and photoluminescence (PL) spectra of MAPQ (film).

semiconductor parameter analyzer. All measurements were performed under ambient atmosphere at room temperature.

Results and discussion

CV measurement was employed to investigate the energy levels of the material. A wave ($E_{\text{onset}}=0.88 \text{ V vs. Ag/Ag}^+$) was observed under an anodic sweep. However, no wave was observed up to -2.60 eV under a cathodic sweep. This is not surprising since many organic materials are more favorable to oxidation rather than to reduction if they are rich in π electrons.¹⁸ The energy value of the highest occupied molecular orbital (HOMO) was calculated to be -5.56 eV by using a ferrocene (FOC) value of -4.80 eV below the vacuum level ($E_{\text{FOC}}=0.12 \text{ V vs. Ag/Ag}^+$).^{19,20}

The energy value of the lowest unoccupied molecular orbital (LUMO) can be estimated from the optical absorption measurement. The UV-Vis absorption and PL spectra of an MAPQ thin film are shown in Fig. 2. The PL spectrum was measured at an excitation wavelength of 395 nm . The absorption consists of a strong $\pi-\pi^*$ transition with a peak at 395 nm and has a relatively narrow linewidth (full width at half maximum $\approx 80 \text{ nm}$). From the extrapolation of the UV-Vis spectrum, the $\pi-\pi^*$ band-gap energy of MAPQ was determined to be 2.70 eV ($\lambda_{\text{onset}}=460 \text{ nm}$). Hence, the energy value for LUMO of MAPQ should be -2.86 eV . The PL spectrum has a maximum at 525 nm .

A single-layer device was fabricated with MAPQ as the emissive layer as shown in Fig. 1(a). When the LED was forward biased with the ITO electrode at positive polarity, yellow-green light emission was observed. The Commission Internationale de L'Eclairage coordinates are $x=0.389$ and

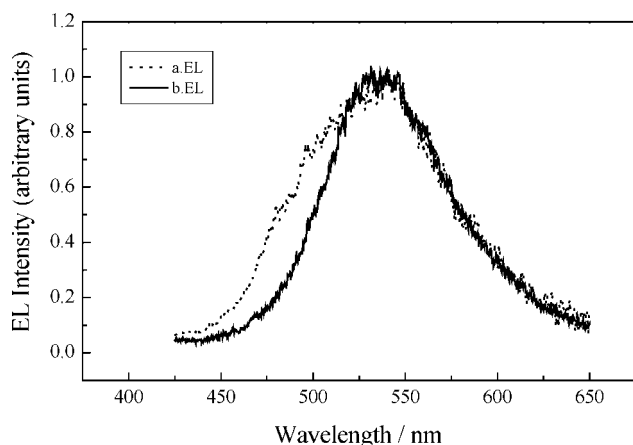


Fig. 3 The electroluminescence spectra of ITO/MAPQ/Al (a) and ITO/TPD/MAPQ/Alq₃/Al (b).

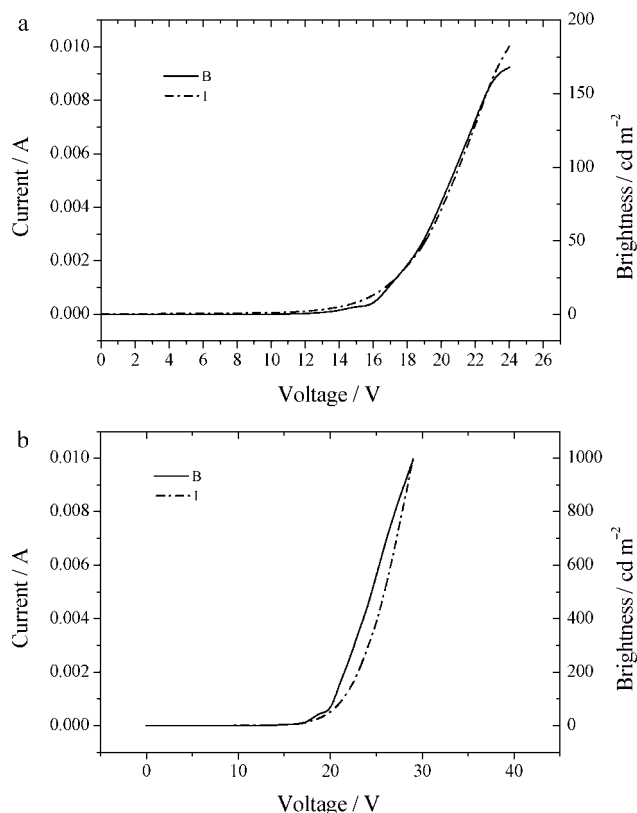


Fig. 4 Electroluminescence intensity and current as function of the voltage for ITO/MAPQ/Al (a) and ITO/TPD/MAPQ/Al (b).

$y=0.530$. The emission spectrum is shown in Fig. 3(a) at a drive voltage of 17 V . The maximum is found to be at 538 nm , which is comparable to that of the PL of MAPQ film, and the spectrum does not change with increasing voltage. It indicates a similar recombination mechanism of charge carriers for the PL and EL of MAPQ, and the emission originates from the radiative recombination of singlet excitons within the MAPQ. Fig. 4(a) shows current-voltage and luminance-voltage characteristics for the device. The $I-V$ curve indicates a diode-like behavior. No light emission has been observed when the reverse bias was applied to the diode structure, *i.e.*, Al was positively biased with respect to ITO. Under the forward bias conditions, *i.e.*, ITO is positively biased with respect to Al, the light emission occurred when the applied voltage was greater than 8 V . The luminance reaches 168 cd m^{-2} at a drive voltage of 24 V and for a current of about 0.01 A .

As sketched in Fig. 5, the energy barrier for electron injection of the single-layer device is about 1.3 eV , while at the anode, the energy barrier for hole injection is about 0.9 eV . Therefore, the energy barrier limits performance of the single-layer device. It is well known that balance and efficiency of charge injection/transport for electrons and holes are crucial for achieving high device efficiency.²¹ So, we

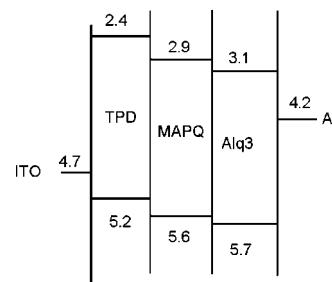


Fig. 5 HOMO/LUMO levels of the TPD, MAPQ and Alq₃ in relation to the work function of the LED.

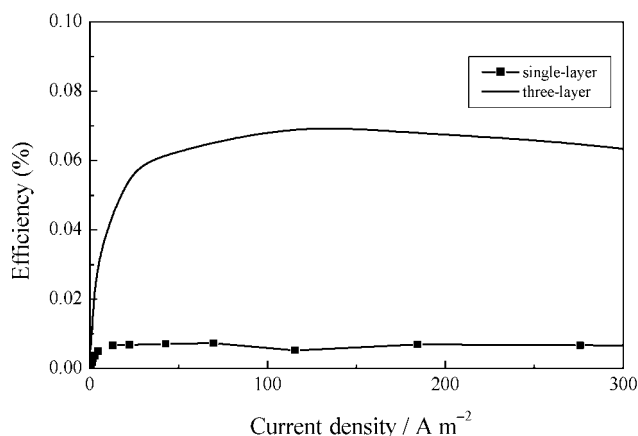


Fig. 6 Efficiency-current density characteristics of ITO/MAPQ/Al and ITO/TPD/MAPQ/Alq₃/Al.

prepared a three-layer device with the structure ITO/TPD/MAPQ/Alq₃/Al. The addition of Alq₃ is to reduce the energy barrier for electron injection and improve its transportation. At the same time we also added TPD in order to increase the hole number in the organic layer to improve exciton production. The energy barriers for electron injection and hole injection reduce to 1.1 and 0.5 eV respectively. The EL spectrum is shown in Fig. 3(b). The EL maximum is similar to that of the single-layer device and located at 538 nm, which indicates the emission originates from the radiative recombination of singlet excitons within the MAPQ, but the EL spectrum at short wavelength is weakened, which makes the spectrum narrow and the light change color from yellow-green to greenish-yellow. The Commission Internationale de L'Eclairage coordinates are $x=0.447$ and $y=0.510$. The current-voltage and luminance-voltage characteristics for the device are illustrated in Fig. 4(b). The device also shows a diode-like behavior. The turn-on voltage (the bias required to give an observed light emission) increases to 11 V, and its luminance reaches 992 cd m⁻² at a drive voltage of 30 V and for a current of 0.01 A. Besides the enhancement of the luminance of the device, the addition of electron-transporting and hole-transporting layers also narrowed the light emission. This result indicates that multilayer devices can be used as a method to narrow the emissions of some materials, whose EL spectrum of single-layer devices is relatively wide.

To compare the performance of these two devices, we calculate the external quantum efficiencies (η_{ext}) by means of eqn. (1):

$$\eta_{\text{ext}} = \frac{n_p}{n_e} = \frac{W/h\nu}{I/eQ}$$

where n_p is the number of the emitted photons per second, n_e is the number of injected electrons per second, W is the luminous power, $h\nu$ is the photon energy, I is the current, and eQ is the electric quantity of each electron. Fig. 6 shows the external quantum efficiencies as a function of current density. From Fig. 6, it is easily noted that at low current density, the increase of external efficiencies in the single-layer device is quite similar to that in the three-layer device. At the initial stage, the efficiency increases very quickly and then slows down with an increase in current density. The maximum η_{ext} increased from about 0.007% in the single-layer device to 0.07% in the three-layer device. It is also worth noting that both of the devices exhibit stability of η_{ext} over a wide range of current densities. From the above discussion, we can deduce that there may be a similar recombination mechanism of charge carriers both for the single-layer device and three-layer devices, and the emission

originates from the radiative recombination of singlet excitons within the MAPQ. The reason for higher efficiencies in the three-layer device is probably efficient carrier recombination in the MAPQ layer because of the relatively balanced and efficient charge injection/transport.

Conclusions

In summary, greenish-yellow PL and EL emission have been demonstrated from a dihydroquinazolinone derivative. By using Alq₃ as the electron injection/transporting layer and TPD as the hole injection/transporting layer, a luminance of 992 cd m⁻² was reached with the maximum η_{ext} of 0.07%. Comparing the performance of single-layer with three-layer devices, we found that the addition of electron-transporting and hole-transporting layers not only improves the luminance of the device, but also narrows the light emission. This implies that a multilayer device can be used as a method to narrow the emission of some materials, while the EL spectra of single-layer devices is relatively wide. These results also demonstrate that MAPQ is a promising candidate for a greenish-yellow emitting organic LED.

Acknowledgements

A Knowledge Innovation Program of the Chinese Academy of Sciences, National Natural Science Foundation of China (69890228, 20082001, 20074032), and the Major State Basic Research Development Program supported this work.

References

- 1 C. W. Tang and S. A. VanSlyke, *Appl. Phys. Lett.*, 1987, **51**, 913.
- 2 J. R. Sheats, H. Antoniadis, M. Hueschen, W. Leonard, J. Miller, R. Moon, D. Roitman and A. Stocking, *Science*, 1996, **273**, 884.
- 3 Z. Shen, P. E. Burrows, V. Bulovic, S. R. Forrest and M. E. Thompson, *Science*, 1997, **276**, 2009.
- 4 R. H. Friend, R. W. Gymer, A. B. Holmes, J. H. Burroughes, R. N. Marks, C. Taliani, D. D. C. Bradley, D. A. Dos Santos, J. L. Bredas, M. Logdlund and W. R. Salaneck, *Nature*, 1999, **397**, 121.
- 5 Y. Shirota, *J. Mater. Chem.*, 2000, **10**, 1.
- 6 L. C. Picciolo, H. Murata and Z. H. Kafafi, *Appl. Phys. Lett.*, 2001, **78**, 2378.
- 7 G. Yu, Y. Q. Liu, X. Wu, D. B. Zhu, H. Y. Li, L. P. Jin and M. Z. Wang, *Chem. Mater.*, 2000, **12**, 2537.
- 8 U. Mitschke and P. Bäuerle, *J. Mater. Chem.*, 2000, **10**, 1471.
- 9 G. Gustafsson, Y. Gao, G. M. Treacy, F. Klavetter, N. Colaneri and A. J. Heeger, *Nature*, 1992, **357**, 477.
- 10 N. C. Greenhan, S. C. Moratti, D. D. C. Bradley, R. H. Friend and A. B. Holmes, *Nature*, 1993, **365**, 628.
- 11 S.-J. Chung, J.-I. Jin and K.-K. Kim, *Adv. Mater.*, 1997, **9**, 551.
- 12 T. Zyung, D. H. Hwang, I. N. Kang, H. K. Shim, W. Y. Hwang and J. Kim, *Chem. Mater.*, 1995, **7**, 1499.
- 13 D. W. Lee, K.-Y. Kwon, J.-II Jin, Y. Park, Y.-R. Kim and I.-W. Hwang, *Chem. Mater.*, 2001, **13**, 565.
- 14 P. R. Bhalla and B. L. Walworth, EP 58822, 1983 (*Chem. Abstr.*, 1983, **98**, 1669).
- 15 H. L. Yale and M. Kalkstein, *J. Med. Chem.*, 1967, **10**, 334.
- 16 M. G. Biressi, G. Cantarelli, M. Carissimi, A. Cattaneo and F. Ravenna, *Farmaco, Ed. Sci.*, 1969, **24**, 199; *Chem. Abstr.*, 1969, **71**, 61357.
- 17 E. Hamel, C. M. Lin, J. Plowman, H. Wang, K. Lee and K. D. Paull, *Biochem. Pharmacol.*, 1996, **51**, 53; *Chem. Abstr.*, 1996, **124**, 134776.
- 18 A. K.-Y. Jen, Y. Q. Liu, Q.-S. Hu and L. Pu, *Appl. Phys. Lett.*, 1999, **75**, 3745.
- 19 Y. Q. Liu, M. S. Liu and A. K.-Y. Jen, *Acta Polym.*, 1999, **50**, 105.
- 20 Y. Q. Liu, H. Ma and A. K.-Y. Jen, *Chem. Mater.*, 1999, **11**, 27.
- 21 M. S. Liu, Y. Q. Liu, R. C. Urian, H. Ma and A. K.-Y. Jen, *J. Mater. Chem.*, 1999, **9**, 2201.